Determination of environmental VOR errors using aerial Doppler cross-bearing measurements

Dr. Thorsten Schrader
Head of Division Mechanics and Acoustics
Physikalisch Technische Bundesanstalt PTB
Baunschweig, Germany
Fax: +49
E-mail: thorsten.schrader@ptb.de

Dr. Thomas Kleine-Ostmann
Head of Department High Frequency and Electromagnetic Fields
Physikalisch Technische Bundesanstalt PTB
Baunschweig, Germany
Fax: +49
E-mail: thomas.kleine-ostmann@ptb.de

Prof. Dr. Jens Werner
Head of RF, Wireless and EMC Lab
Jade University of Applied Sciences
Wilhelmshaven, Germany

E-mail: jens.werner@jade-hs.de

Karsten Schubert M.Sc.
PhD student, RF, Wireless and EMC Lab
Jade University of Applied Sciences
Wilhelmshaven, Germany

E-mail: karsten.schubert@jade-hs.de

SECOND AUTHOR PHOTO HERE

Prof. Dr. Jochen Bredemeyer
Head of research
Flight Calibration Services FCS GmbH
Braunschweig, Germany
Fax: +49
E-mail: brd@fcs.aero

Dr. Ralf Eichhorn
CNS expert
Deutsche Flugsicherung DFS GmbH
Langen, Germany
Fax: +49
E-mail: ralf.eichhorn@dfs.de

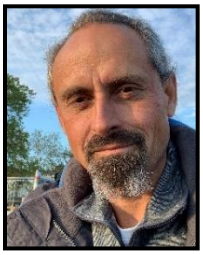

ABSTRACT

Future airspace usage and procedure design will be based on area navigation and PBN operation. While the primary sensor for this is GNSS, several fall-back systems have to be provided which rely on terrestrial facilities, some of them being VORs. Accordingly, ANSPs have to decide whether a certain VOR supports RNAV-5 or not. Within conventional procedures, the performance is ensured by means of flight inspection but there is no good solution how to guarantee signal integrity virtually everywhere.

Our approach could contribute to improve this situation and to gain insight into signal in space on signal level. For this purpose, a new bandpass receiver technology and digital board is used to obtain measurement data of signal in space and to store that data synchronized with GPS time stamp and location on SSD. The electronics is either carried using PTB's octocopter or the touring motor glider JadeOne (D-KWHV). Applying the new Doppler cross-bearing method one is able to locate each scatterer around the DVOR and, furthermore, to determine its associated reflectivity. This clutter map can be used as a preload Az-Error in the VOR protection area, but, furthermore, it is possible to calculate the scatterers' impact on the DVOR signal integrity as well as the impact of wind turbines up to the VOR range limit.

Our measurements and analysis confirmed that simple orbital data from flight inspections are not adequate to judge on the preloading Az-Error that exists due to the multipath environment. Physical and metrological reasons that support existing regulations (for example by the FAA) were identified which preclude facility restrictions solely based on orbit inspection data.

Originally aiming at refining the assessment of wind farm projects and their impact on area navigation, the scope of our findings could be expanded. Based on the clutter maps derived from measured data a method was developed that allows predicting VOR azimuth errors at almost every point in space. By that means one is able to document RNAV compliance. Furthermore, our method can also be used to predict, whether a newly constructed conventional procedure will comply with DOC 8071 requirements even bevor flight validation has taken place.

INTRODUCTION

In addition to error contributions of new wind turbines, bearing errors of the so-called preload $\Delta\varphi_{Vorbelastung}$ have to be considered for the prognosis. This includes all objects in the operational range of the VOR that are illuminated according to its effective antenna diagram. Here, shadowing, e. g. by woods, but also diffraction, scattering and reflection of electromagnetic waves can be relevant. The bearing error caused by such an obstacle extends into free-space similar to an optical projection and reaches heights that are used by air traffic.

ICAO distinguishes between fast (Scallops) and slow (Bends) spatial fluctuations of the bearing error. Due to inertia, air planes can follow Bends, only. These are the only ones that could impair correct navigation. Therefore, ICAO DOC 8071, I-2.3.12 and I-2.3.48 mandates the evaluation of Bends on radials by flight inspection, with flight maneuvers where the bearing angle towards the VOR remains constant. These flight inspections are done periodically in order to ensure the validity of signals and installations close to airports.

The DFS preload analysis so far is based on orbital flight inspections that are originally meant to adjust the north alignment of VORs, only. While results from radial flight inspection maneuvers have the tendency to remain constant over years, orbital flight inspection results fluctuate from year to year. The underlying data appears to be significantly noisier than in the case of radial measurements. A comparison of orbital and radial measurement data at intersection points is not available, so far. There is also an FAA order [1] that warns about overinterpretation of orbital flight data.

Radial flight inspection measurement data shows Bends at radial distances exceeding 10 nautical miles in the form of sinusoidal fluctuations over radial distance. Measuring the bearing error at a fixed radial distance, as in the case of an orbital flight, does not allow to determine the magnitude of the fluctuation, since only a single, arbitrary point of the fluctuation is sampled. In addition, during an orbital flight, the orientation of the measurement antenna of the airplane (V-dipole at the cockpit roof) is not suitable to measure properly a horizontally polarized field originating from the VOR, since antenna and field orientation are mostly orthogonal. This explains the noisy character of orbital flight inspection measurements. In order to cope with this noisy data, DFS used a sliding window of +/- 4.5° considering the 95 % percentile of measurement values, only. Most recent plans of DFS foresees the use of arbitrary flight maneuvers instead of orbital flight, however, it remains questionable how this data can contribute to a reliable estimation of the preload.

Within the project "WERAN plus" a new method for preload analysis using Doppler-cross bearing [2] is proposed that is based on a more scientifically appropriate physical approach. It allows to consider arbitrary interferers (reflecting objects such as

trees, buildings, high-voltage power lines and already existing wind turbines) with regard to location and interference potential. The resulting clutter map [3] can be included into the prognosis calculation to estimate the already existing bearing error due to the preload and to combine it with the bearing error expected by newly built additional wind turbines. This improves aviation safety significantly, as high building at a distance exceeding 3 km to the VOR and high-voltage power lines have not even been part of the safety analysis.

Hybrid Bearing Error Prognosis

As part of WERAN plus, the new approach based on Doppler cross-bearing has been developed. The identified scatterers can be interpreted as equivalent sources that radiate the interfering fields. Figure 1 depicts the principle: a complex environment with numerous scatterers is replaced by a simplified model of the environment and deviating properties are modeled with additional interferers. Additional wind turbines that are to be built can be included, easily, by placing their equivalent source into the model. This way, based on a preload measurement in form of a clutter map, a much more realistic modelling of the overall problem is possible. The interfering potential of a scatterer depends on the distance to the DVOR, but also from the height and dimension of the object. Hence, small but close objects such as trees can have a similar interference potential as large buildings or high-voltage power lines located far from the DVOR.

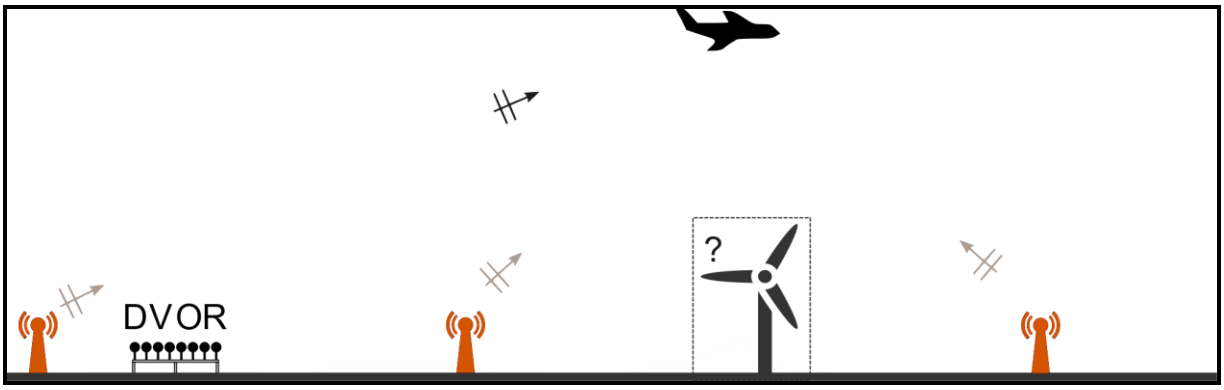

Figure 1. Simplified Model Environment with Additional New Wind Turbine [1]

SIMILARITY TO RADAR APPLICATION

In this paper, the usage of a Passive Bistatic Radar (PBR) application to generate a ground clutter map in the VHF navigation band is described. These clutter parameters are finally used to populate a set of linear coefficients in a process in order to forecast the signal degradation of an aircraft navigation facility. That requires a combination of both, the given preload of existing scatterers and additional objects to be erected in a building restricted area. The outcome is an important contribution to solve a long-term conflict in context with in the construction of wind power plants. However, the focus here is mainly on the Radar-related aspects of localization and quantization of scatterers on the ground as an essential prerequisite.

A transmitter of opportunity for PBR is usually from a non-radar transmission that has no further cooperative signal properties to facilitate the target localization. In this case however, a Doppler-VOR (DVOR) transmitter is used that inherently radiates a directional information. The new localization process described makes use of differential Doppler shift due to aircraft motion and of the directional information of the scattered VOR signal. The theory and some promising measurements result will be shown.

METHODOLOGY

The localization of reflecting objects is based on cross bearing that needs two distinct angular values. One is derived from the modulated signal itself that is transmitted by a DVOR pointing to the reflecting object. The other is concluded from Doppler shift analysis of the reflected signal. The following paragraphs describe this process in more detail.

Data Acquisition

The electromagnetic field of the DVOR transmitter is received airborne and fed into a software defined radio receiver (SDR). The SDR converts the radio frequency (RF) signal to a lower intermediate frequency (IF). An analog-to-digital converter (ADC) finally provides complex IQ data samples which are stored on an external computer. All internal clock signals as well as local oscillator frequencies are fully coherent with a single high precision reference clock (Oven Controlled Crystal Oscillator (OCXO) locked onto GPS time reference).

Correction of Transmitter Frequency Deviation

An unwanted momentary frequency deviation of up to ±20 Hz was observed for carrier of the investigated DVOR transmitter Bremen (BMN), f_c = 117.45 MHz). This impedes the analysis of any Doppler shift caused by the velocity of the measurement aircraft. Hence, a second SDR set, locked to another OCXO/GPS reference was placed close to the DVOR transmitter, allowing a quasi-coherent data acquisition of ground-based and airborne RF signals. Post-processing of these two data sets removes the unwanted transmitter frequency deviation, compensates for Doppler frequency shift from radial movement of the aircraft towards the DVOR and yields a new complex base band signal with following properties:

- Centered to 0 Hz (i.e. the formerly unstable RF carrier is permanently shifted to 0 Hz
- Data samples are complex valued, preserving negative and positive frequency
- AM reference signal of DVOR is at -30 Hz and +30 Hz
- FM sub-carrier of DVOR signal is located at -9960 Hz and +9960 Hz
- Spectra of FM sub-carrier show Bessel line-spectrum (N•30 Hz)

Fig. 2 shows the base band spectrum of a received signal from direct line of sight propagation. In presence of reflecting objects additional signals would be superimposed that exhibit a small Doppler shift since they arrive from a different angle at the airborne receive antenna. This shift allows the separation of multiple signals by means of cross-correlation as explained below.

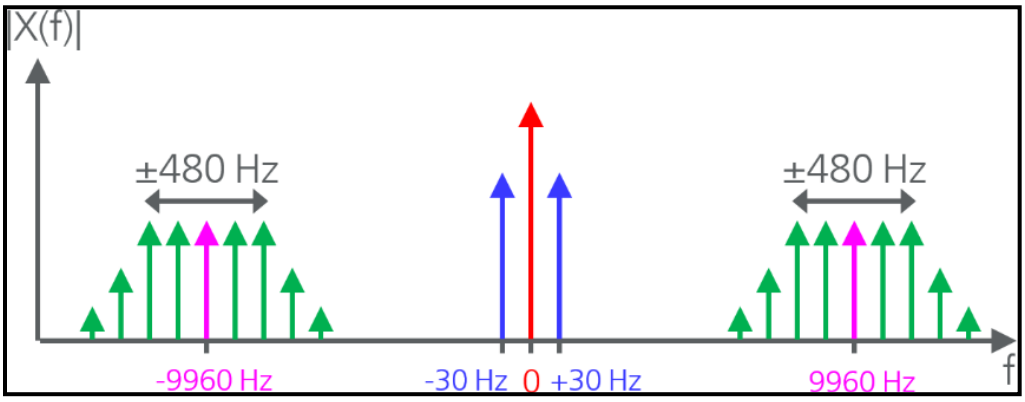

Figure 2. Nominal Baseband Spectrum of a Doppler VOR.

FM-Demodulation based on Cross-Correlation

A measurement flight results in a large number of data samples *y(t),* (flight time • sampling rate • sample size • channel count, e.g. 60 min • 96 kS/s • 8 Byte/S • 2 = 6.9 •10^8 S • 8 Byte/S = 5.5 GByte). Those samples are cross correlated with a complex test function x(t) that represents an ideal FM signal in the time domain:

$$x(t) = e^{+i\cdot 2\pi (f_d + 9960\ \mathrm{Hz})t} \cdot e^{+i\cdot \eta \sin(2\pi 30\ \mathrm{Hz}\cdot t)} \quad (1)$$

Where f_d is the expected Doppler shift and η is the FM modulation index. The length of this test function is selected to cover more than a single period in order to increase the spectral resolution and finally accuracy when testing for the exact Doppler shift (e.g. 1 min. allows <0.1 Hz resolution band width (RBW)). Given the huge number of data samples, performing the cross correlation is computationally expensive. Here, the implementation is applied in the frequency domain:

$$r_{xy}^{E}(\tau) = \int_{-\infty}^{\infty} x(t) \cdot y(t+\tau)\,dt \quad \circ\!\!-\!\!\bullet \quad X^{*}(j\omega) \cdot Y(j\omega) \tag{2}$$

The combination of equations (1) and (2) resembles the well-known ambiguity function (AF) that represents the time response of a Matched Filter to a finite signal when the signal is received with a delay τ and a Doppler shift f_d [4].

Both, the test function x(t) and the base band samples *y(t)* are converted by fast Fourier transformation (FFT) into the frequency domain and simply multiplied element by element. The resulting data is finally processed by inverse FFT and yields the complex valued correlation data. This procedure is repeatedly performed for any Doppler shift under investigation. E.g. to cover Doppler shift frequency f_d from -15 Hz to +15 Hz with steps of 0.1 Hz, 301 steps are required (Matlab runtime on a dual XEON workstation is 20 hours).

For the test function *x(t)* used here, the impulse response is identical ($x(t) = x^{*}(-t)$). A Gaussian window is applied, so that the final impulse response becomes:

$$h(t) = \sqrt{\frac{\alpha}{\pi}} \cdot e^{-(\alpha t)^2} \cdot e^{+i \cdot 2\pi (f_d + 9960\ \mathrm{Hz})t} \cdot e^{+i \cdot \eta \sin(2\pi 30\ \mathrm{Hz} \cdot t)}$$
$$\alpha = \frac{20\pi^2}{\ln(10)} \cdot \frac{{f_{RBW}}^2}{A_{dB}} \tag{3}$$

Here, f_{RBW} denotes the resolution bandwidth of the resulting comb filter and A_{dB} is the stop band attenuation in decibel. The Fourier transform $H(j\omega)$ of this impulse response is depicted in Fig. 3.

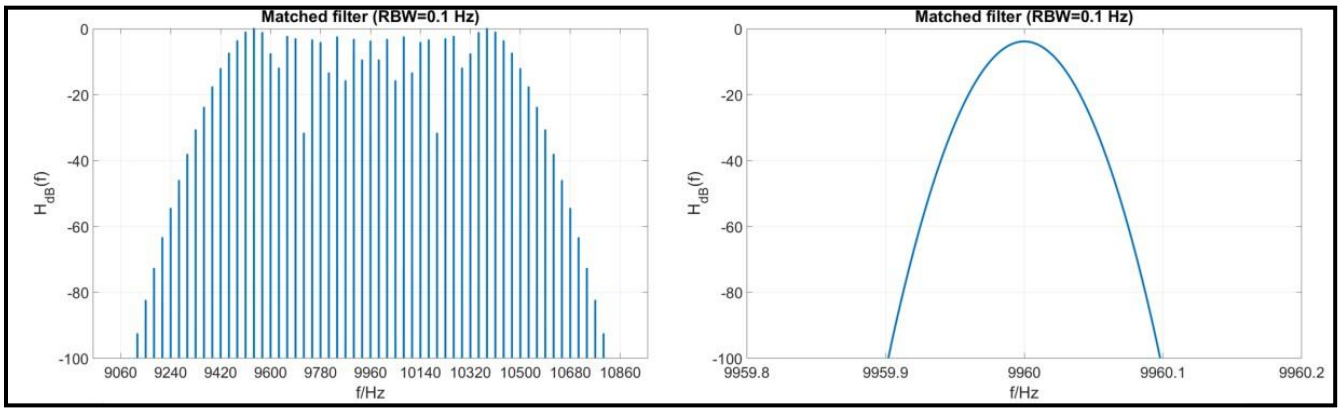

Figure 3. Left: FFT of Test Function results in Comb Filter, Envelope is shaped by Bessel Coefficients of FM, right: Detail of a single „line" from the Comb Filter, RBW is 0.1 Hz

Probing into to the comb filter characteristic of the Fourier transform $H(j\omega)$ another explanation for this procedure can be given: A comb filter with Bessel shaped envelope (Matched Filter) is slid over the Bessel spectrum of the investigated Doppler spectrum. This provides correlation coefficients for each sampling point in the time domain (2D convolution: time and Doppler shift). A maximum in the correlation provides the time for a reflection. The phase of the DVOR AM reference signal at exactly this time provides just the radial directed from the DVOR to the reflecting object (see Fig. 4). This is the first step for localization of the reflecting object by means of cross bearing. The cooperative DVOR transmitter inherently modulates this bearing information onto the signal which it is sent towards the reflecting object.

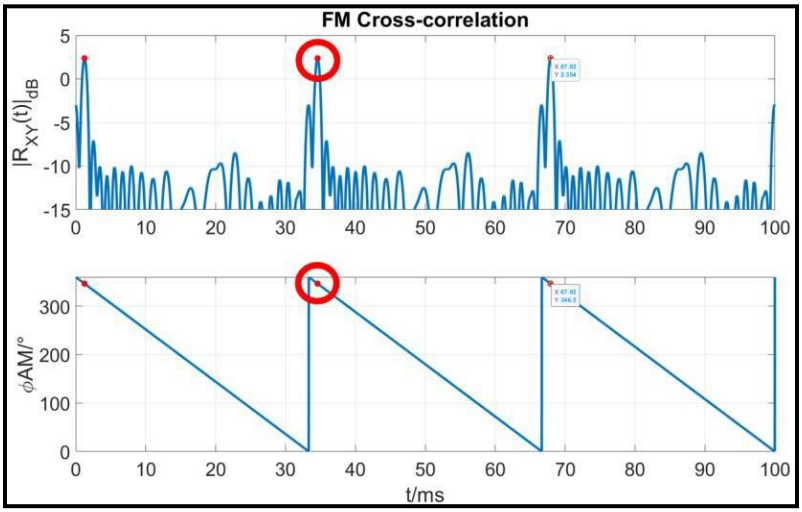

Figure 4. Magnitude of Correlation Data (top) and Phase Information from D-VOR AM Reference (bottom).

Calculation of Second Bearing from Doppler Shift of Reflected Signal

Due to known position, velocity, and heading (GPS+IMU) of the aircraft, the angle between the aircraft movement and the scatterer can be calculated from the radial velocity component relative to the scatterer and its resulting Doppler shift. This is the second step for the cross bearing. The Doppler shift f_d is proportional to the sine of the angle a (see Fig. 5), with DVOR carrier frequency f_c, speed of light c_0 and ground speed v of aircraft:

$$f_d = f_c \frac{v}{c_0} sin(\alpha) \tag{4}$$

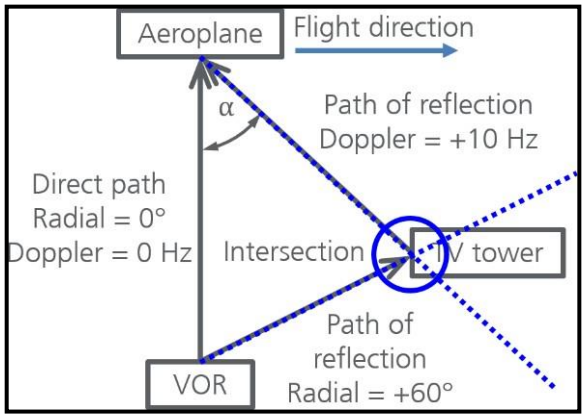

Figure 3. Example of Geometry: The DVOR Signal towards the Reflecting TV Tower is Modulated with Bearing Angle 60°, this Signal arrives at the Aircraft with Incident Angle α and hence causes 10 Hz Doppler Shift.

Calculation of Quasi Radar Cross-Section

According to [4] the incident field is assumed to be planar over the extent of the target. This is in principle not the case for objects on the ground. Hence, these results here are referred to as a Quasi-RCS. Using Friis´ equation for free space propagation loss [3] the received power $P_{Rx,d}$ from **d**irect path of propagation can be expressed as product of power flux density S_d and airborne receive antenna aperture $A_{W,Rx}$:

$$P_{Rx,d} = \overbrace{\frac{P_{Tx} G_{Tx}}{4\pi {R_d}^2}}^{S_d} \cdot \overbrace{\frac{\lambda^2 G_{Rx}}{4\pi}}^{A_{W,Rx}} \tag{5}$$

By applying the Radar equation [4] the power $P_{Rx,S}$ that is received from the **s**cattering object is given as:

$$P_{Rx,s} = \overbrace{\frac{P_{Tx}G_{Tx}}{4\pi {R_t}^2}}^{S_t} \cdot \overbrace{\frac{\sigma}{4\pi {R_r}^2}}^{S_r} \cdot \overbrace{\frac{\lambda^2 G_{Rx}}{4\pi}}^{A_{W,Rx}} \tag{6}$$

Here, the power flux density S_t denotes the power transmitted **t**owards the scattering object with antenna gain G_{Tx} of the VOR transmit antenna and distance R_t to the object. S_t gives the power flux density at the location of the aircraft derived from RCS σ of the scattering object in distance R_r. This can be solved for σ and results in:

$$\sigma = 4\pi \frac{P_{Rx,s}}{P_{Rx,d}} \cdot \frac{{R_t}^2 {R_r}^2}{{R_d}^2} \tag{7}$$

For large distance, i.e. $R_d >> R_t$ and $R_d \approx R_r$ this can be approximated by:

$$\sigma \approx 4\pi \frac{P_{Rx,s}}{P_{Rx,d}} \cdot {R_t}^2 \tag{8}$$

In this derivation, free space propagation was assumed while any real environment is located close to a ground and entails many objects, like buildings, trees, and so on. Thus, the derived RCS is regarded as quasi value, allowing to generate the wanted clutter map of various objects showing different reflection coefficients.

MEASUREMENTS

In Fig. 6 a typical flight maneuver is shown that was carried out near Bremen airport using a motor glider. The Doppler VOR as PBR source is directly located at the airport. Some results from this flight are shown.

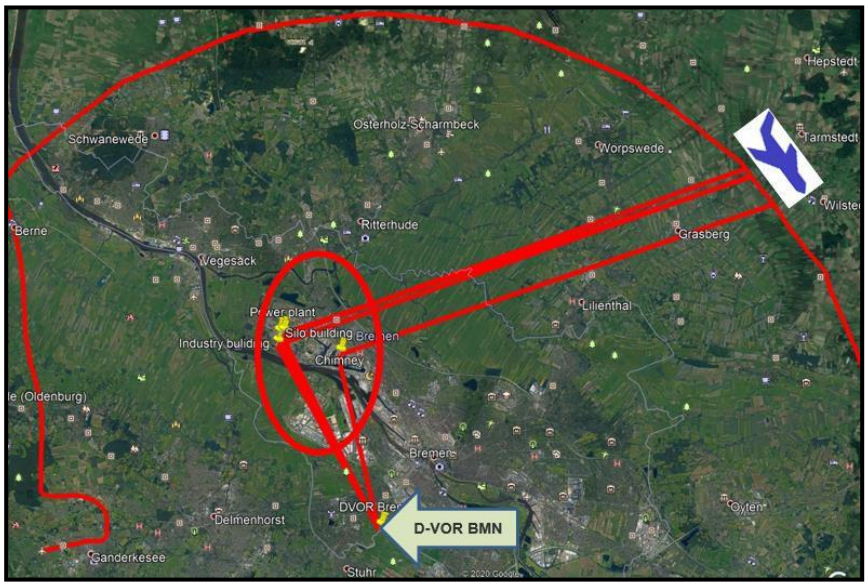

Figure 6: Orbit Flight around Bremen Airport where PBR Source „DVOR BMN" is located (Image Source: Google Earth)

Based on the algorithm derived in previous section, it is possible to generate a clutter map with real objects that surround the VOR location. The intersections of cross bearing with their respective reflection strengths (color) are given in Fig. 7 (right).

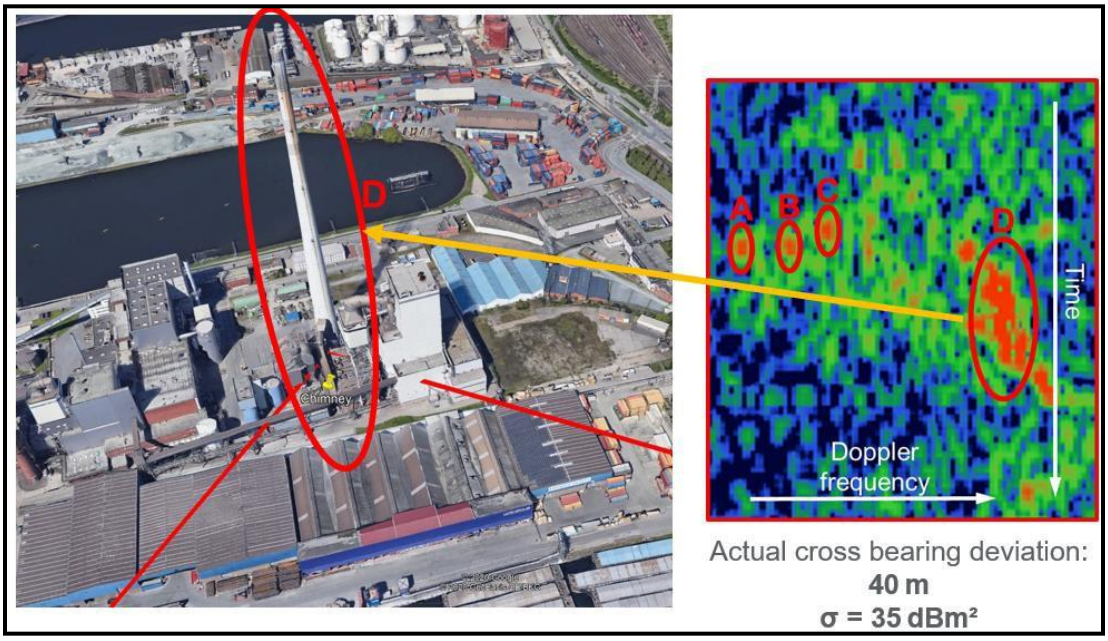

Figure 7: Cross Bearing Result as of Detected Chimney (D) with Assigned Quasi-RCS

Combining these results with satellite images one can easily allocate the localization result (D) to an existing building ensemble (left). A chimney is the highest object that represents a quasi-RCS of 35 dBsm.

The entire graphic evaluation of the cross bearing results provides the clutter map depicted in Fig. 8. Above a threshold of 15 dBsm, this map reveals in >95% of all cases objects like skyscrapers, chimneys, wind turbines, power plant, TV towers or similar objects.

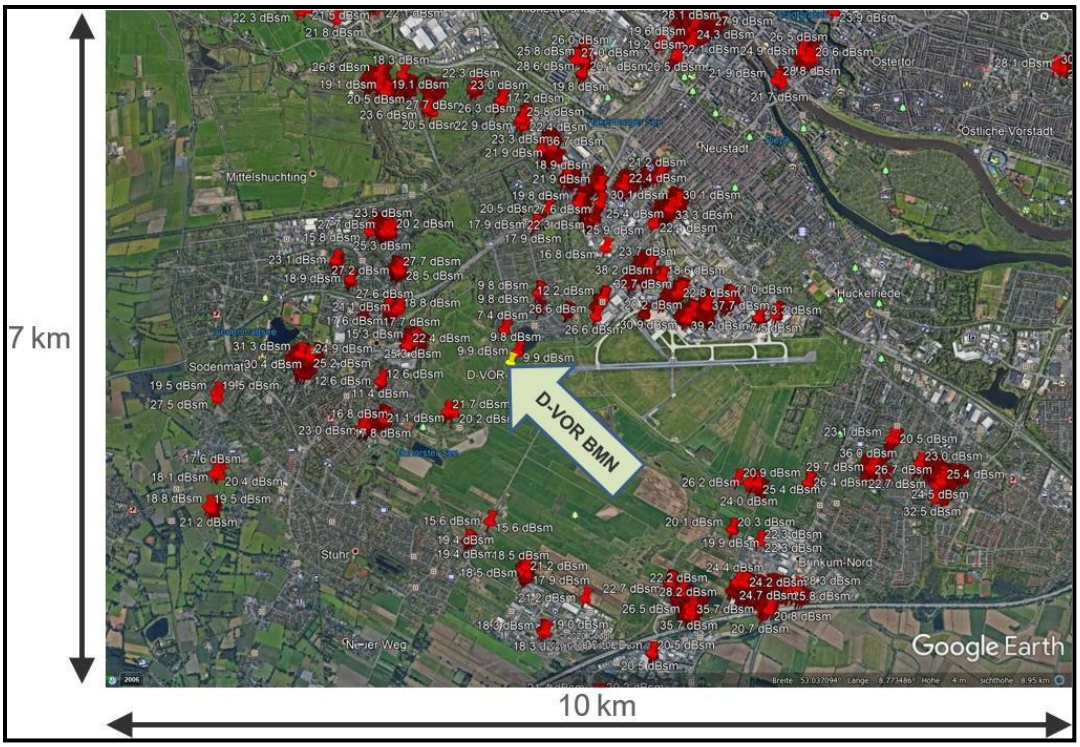

Figure 8: Ground Clutter Map of various Objects with Quasi-RCS Values above Threshold (Image Source: Google Earth)

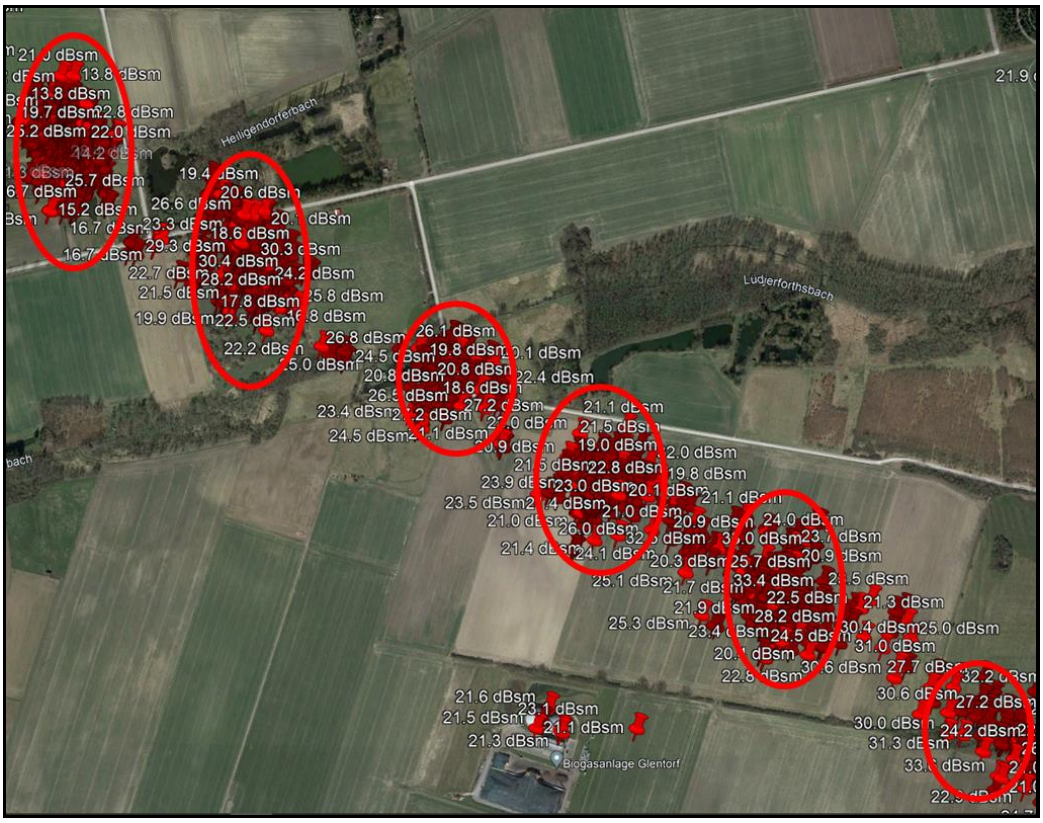

Figure 9: Clutter Map showing Location and Reflectivity of Power Pylons, 750 m distant to DVOR Hehlingen (HLZ), (Image Source: Google Earth).

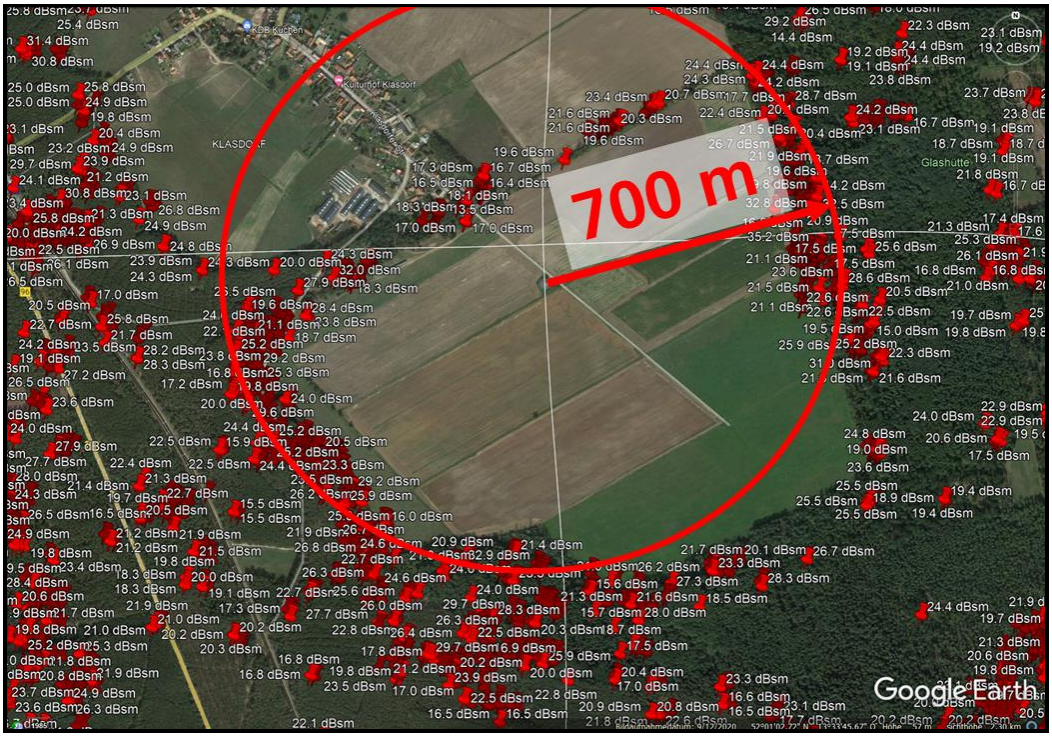

Figure 10: Clutter Map showing Location and Reflectivity of Reflecting Objects near DVOR Klasdorf (KLF), (Image Source: Google Earth).

Fig. 9 depicts reflecting objects close to DVOR Hehlingen. From satellite images those objects can be identified as power pylons. Markers as result from Doppler cross-bearing method are nicely grouped around the actual position of the pylons.

In Fig. 10 data from measurements at DVOR Klasdorf are shown in a clutter map. The VOR is located at the centre of the red circle. No objects were detected over the plane field area. Adjacent to those fields trees from forest area causes significant reflections. Some trees cause reflections similar in strength to those of power pylons.

PREDICTION OF THE BEARING ERROR

Based on the clutter maps obtained as described above, we will now predict the bearing that will exist in any point in space. The approach that will be used is depicted in Fig. 11: We assume the VOR being a simple radio source. At any point in space (symbolized by the aircraft in Fig. 11), we can calculate the power flux density (PFD) of the direct signal, for example by means of free space path loss. In the same manner, the PFD of any multipath signal can be calculated if the reflectivity of any scatterer is characterized by its (bistatic) radar cross section RCS. Eventually, the field strength of each signal at any point in space can be calculated.

To predict the bearing error under multipath conditions an analytical receiver model is used, which is taken from [8], based in the initial work in [9]:

$$\epsilon = \mathrm{Arctan}\left(\frac{2\sum_{n=1}^{N} \frac{a_n}{a_0} \times \cos(\Phi_n - \Phi_0)\, J_1\left[2\, m_f \sin\left(\frac{\theta_n - \theta_0}{2}\right)\right] \cos\left(\frac{\theta_n - \theta_0}{2}\right)}{m_f + 2\sum_{n=1}^{N} \frac{a_n}{a_0} \cos(\Phi_n - \Phi_0)\, J_1\left[2\, m_f \sin\left(\frac{\theta_n - \theta_0}{2}\right)\right] \sin\left(\frac{\theta_n - \theta_0}{2}\right)} \right) \tag{9}$$

where a_0 and a_n are the amplitudes of the direct or the n-th indirect fields, ϑ_0 and ϑ_n are the RF (carrier) phase of the direct or the n-th indirect signal, φ_0 and φ_n the azimuth angles of the observer and the n-th scatterer, m_f the FM modulation index (=16 for a VOR) and finally J_1 the 1st order Bessel function.

Our model allows us to calculate the amplitudes of all signals (direct and multipath), the cluttermap gives us the azimuth of every scatterer (with respect to the VOR location), the reflectivity in terms of the RCS- Finally the RF carrier phases can be calculated based on geometric path length calculations so eventually all parameters that go into eqn. (9) are known, so the bearing error can be computed.

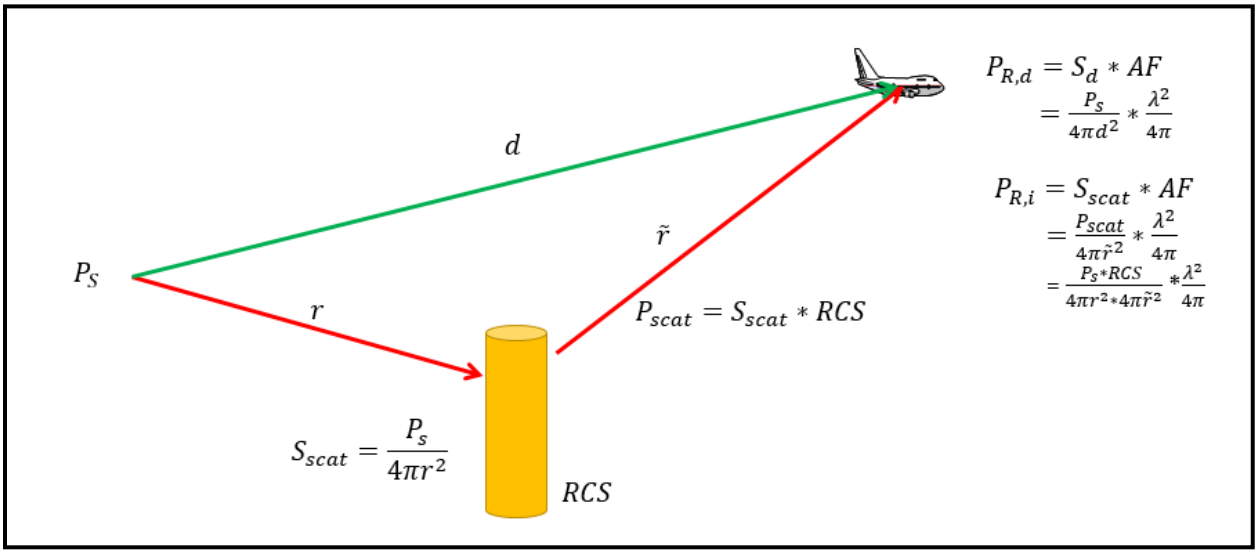

Figure 11: Bearing Error Prediction Based on the quasi-RCS and the Propagation Paths. Based on the Power of the Direct and Indirect Signal an Amplitude Ratio can be Calculated.

The outcome of that calculation is shown in Fig. 12, where VOR bearing error, based on the measured clutter map, along an orbit at 60 NM has been calculated. This is just one example, as the method itself is not restricted to a certain flight pattern. Accordingly, bearing errors a long a radial can also be determined. In conjunction with the filtering techniques described in DOC 8071 virtually all radials can be assessed and a true RNAV compliance can be assured.

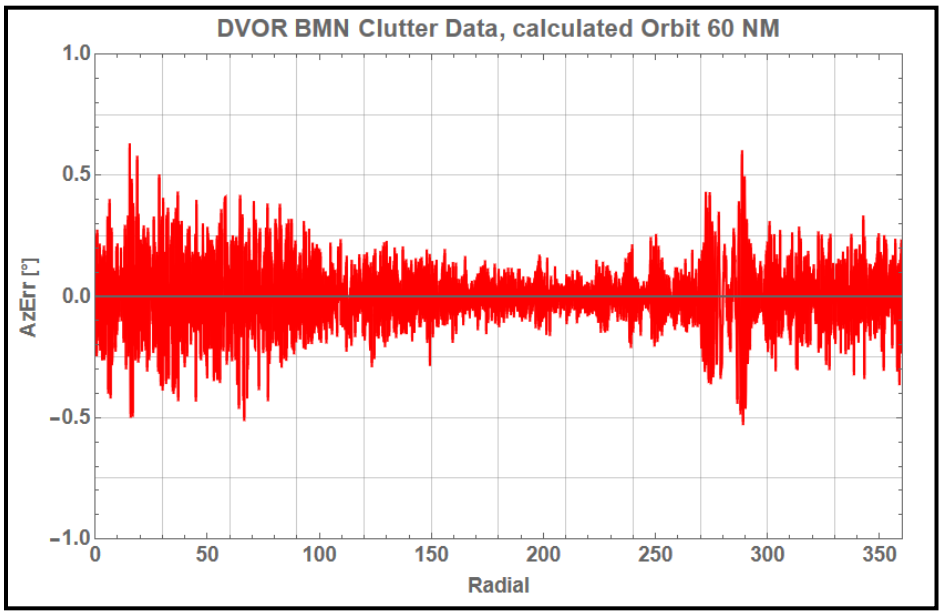

Figure 12: Predicted Bearing error along a 60 NM Orbit.

It is one of the great advantages of the measurement and prediction technique that an assessment of the signal accuracy can be made even at locations where there was no flight data taken. Based on the clutter map one could draw areal heat maps and identify regions with increase bearing errors.

CONCLUSIONS AND ONGOING WORK

A new PBR-based method is presented that can be used to compute a ground clutter map for air navigation VHF band. It makes use of a DVOR transmitter that is partially cooperative to provide an additional component for localization of objects on ground.

There will be carried out an intensive measurement campaign starting this year to generate these ground clutter maps for all operational Doppler VOR facilities in Germany. This will be part of a reliable forecast method to predict the VOR bearing signal degradation of new buildings, especially wind turbines, within building restricted areas.

ACKNOWLEDGMENT

This work was supported by the “WERAN plus” research project (support granted by the Federal Ministry of Economy and Energy according to a resolution by the German Federal Parliament, FKZ: 0324252).

REFERENCES

[1] FAA Order 8200.1D - US Standard Flight Inspection Manual (USSFIM) Chap. 11. Sect. 4. f. (1)(d)

[2] K. Schubert, J. Werner und J. Bredemeyer, „Localisation and Characterisation of Scatter Objects using VHF channel sounding“, in Specialist Meeting on Electromagnetic Waves and Wind Turbines 2021 (EMWT 2021), Zürich, Schweiz (online), 2021

[3] K. Schubert, J. Bredemeyer und J. Werner, „Generation of VHF ground clutter map employing partially cooperative transmitter“, in 2021 21st International Radar Symposium (IRS), pp. 1-10, doi: 10.23919/IRS51887.2021.9466199, 2021.

[4] IEEE Std 211-1997: IEEE Standard Definitions of Terms for Radio Wave Propagation. https://ieeexplore.ieee.org/servlet/opac?punumber=5697

[5] N. Levanon ; E. Mozeson: Radar Signals.; John Wiley & Sons, 2004

[6] H. T. Friis, "A Note on a Simple Transmission Formula," in Proceedings of the IRE, vol. 34, no. 5, pp. 254-256, May 1946, doi: 10.1109/JRPROC.1946.234568.

[7] H. T. Friis and W. D. Lewis, "Radar antennas," in The Bell System Technical Journal, vol. 26, no. 2, pp. 219-317, April 1947, doi: 10.1002/j.1538-7305.1947.tb01317.x.

[8] S. Ben-Hassine. Multipath and receiver models for assessing the VOR bearing error: application to wind farms. Signal and Image processing. Dissertation, Université Paul Sabatier - Toulouse III, 2020, https://tel.archives-ouvertes.fr/tel-03001293

[9] S. Odunaiya und D. Quinet, „Calculations and analysis of signal processing by various navigation receiver architectures," in Digital Avionics Systems Conference, Athens, Ohio, 2004